Acta Scientific Orthopaedics (ISSN: 2581-8635)

Volume 5 Issue 9 September 2022

Research Article

Establishment of a Finite Element Model and Biomechanical Analysis of Different Fixation Methods for Total Talar Prosthesis Replacement

Qian Dong Yang, Le Chang, Xuting Bian, Lin Ma, Kang Lai Tang and Xu Tao*

The First Affiliated Hospital of Military Medical University of the Army, China

***Corresponding Author:** Xu Tao, The First Affiliated Hospital of Military Medical University of the Army, China.

DOI: 10.31080/ASOR.2022.05.0556

Received: July 12, 2022

Published: August 22, 2022

Abstract

As a new technology, three-dimensional (3D)-printed personalized talar prostheses are fixed via different methods, including fixing the subtalar joint and talonavicular joint with screws and fixing only the subtalar joint with screws and fixation without screws. No biomechanical study has been conducted yet. We aimed to build a 3D finite element model to compare the biomechanical effects of different fixation methods. With 3D CT and MRI data of a volunteer's foot, Mimics research 19.0 and Geomagic wrap 2017 software were used to complete the geometric reconstruction of bone and cartilage, and then the data were input into NX12.0 software to build finite element models. Finally, the models were imported into Abaqus 6.14 software for meshing and assigning material properties and for simulating the different biomechanical characteristics in three gait phases. The pressure changes in the articular surface around the talus or the prosthesis, the micromotion of the talus and the prosthesis and ankle motion were measured. The 3D finite element model created in this study has been verified to be consistent with those in previous studies. The results showed that screw fixation of the prosthesis in different gait phases mainly increased the pressure on the tibial-talus articular surface and decreased the pressure on the fused articular surface and joint micromotion, which may hinder ankle motion. The indicator values were nearly the same in the models of fixation without screws and the healthy state. Fixation of the prosthesis without screws yielded values most similar to healthy values.

Keywords: Talar prosthesis replacement; Biomechanical analysis; Finite element

Introduction

Level of Clinical Evidence 5

The talus is the key bony structure connecting the lower limb and foot, and it is the mechanical point of rotation between the lower limb and foot. Stress is concentrated in this area, and the mechanical properties are particularly important [1-3]. Collapsible talus necrosis severely affects individuals' ability to stand and walk, with a disability rate of 100%. Ankle surgeons worldwide mainly perform total talus removal and partial joint fusion at the expense of talar function. Postoperative complications such as adjacent joint degeneration, joint stiffness, and the loss of foot flexibility often occur, and the long-term efficacy of this method is very poor [4,5].

Due to advancements in modern three-dimensional (3D) printing and prosthesis casting technology [6], 3D-printed personalized talar prostheses have been used for clinical treatment [7-10], considerably improving the treatment for talus collapse necrosis worldwide. The surgical indications for prostheses are very similar to those used for conventional methods, but the method of prosthesis fixation is different. In previous studies by Kadakia., *et al*.

[11] and Tracey., *et al*. [12], the peritalar soft tissue was directly removed without fixation of the talar prosthesis with screws. In studies conducted in China, the prosthesis was fixed to the calcaneus using screws [13], or the prosthesis was screwed to both the calcaneus and navicula. However, no biomechanical studies have been performed on the above fixation methods for total talar prostheses.

Finite element analysis (FEA) is a new technology that can be used to establish a mathematical model with high similarity in reflecting regional mechanical characteristics. The greatest advantage of FEA is that it can be used to obtain research results that are difficult to acquire in objective human or animal experiments without causing damage [14,15]. Regarding ankle joint motion mechanics and the gait cycle, the heel-strike phase, midstance phase and push-off phase represent the support and swing phases of the gait cycle and are the three periods that best reflect a healthy gait and pathological function. Therefore, these three phases have been simulated to measure the stress and micromotion of the joints around the whole talar prosthesis as well as ankle joint motion [16,17].

In this study, we used the finite element method to explore the characteristics of the whole talar prosthesis under different fixation methods to compare the biomechanical effects of different fixation methods.

Materials and Methods

Data collection

A male volunteer aged 30 years with a height of 177 cm, a body weight of 75 kg and a foot length of 250 mm participated in planning left artificial talus replacement in this study. An X-ray examination of the right ankle was performed first to exclude other diseases, such as foot tumors and deformities. A 64-slice spiral CT scan (spatial resolution is 30 Lp/cm) of the right ankle was performed, with a slice thickness of 0.60 mm, and MRI was performed to verify the cartilage boundaries. The data were output and saved in DICOM format. In addition, we collected MRI data of the right foot of additional volunteers to help determine the cartilage boundaries.

Finite element model establishment

The CT scan data were imported into the 3D reconstruction software Mimics 19.0, and the bone tissue and soft tissue were separated (thresholding, split masking, region drawing) to establish a geometric model of the whole foot, which was output as an STL file. Then, this file was imported into the reverse engineering software Geomagic Wrap 2017, removing the noise of the model and smoothing the model. According to the geometric shape of each joint surface, the cartilage boundary was divided on each bone surface, the surface was fitted, and the resulting file was output in the Stp format. Then, it was imported into the finite element preprocessing software NX12.0 to build different models. Next, the models were imported into ABAQUS 6.14 software. Based on the ligament data, a model with ligaments was established by connecting the ligament attachment points with the 3D arrangement of the fiber bundles. Finally, the solid model was subjected to mesh generation, material attribute selection, and other processing steps (Figure 1).

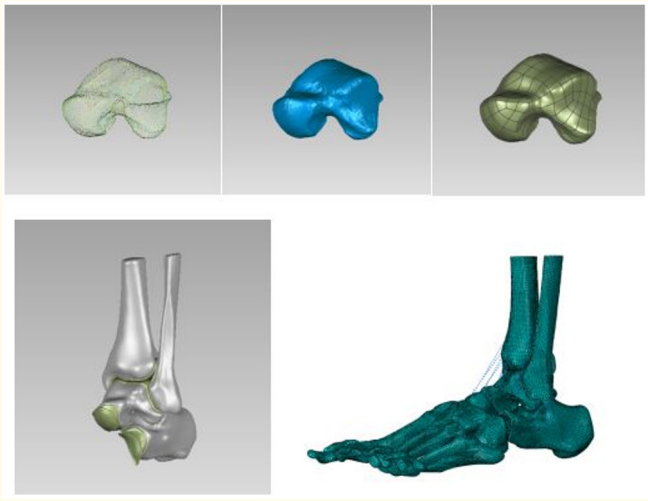

Figure 1: Schematic diagram of the finite element modeling process.

Material parameters

The bony structures and cartilage were modeled as isotropic linear elastic materials, and the ligaments had a nonlinear single-axis connection unit to simulate the characteristics of tension only without compression. The material properties of the bones, cartilage, titanium alloy and ligaments were determined according to previous studies and are listed in tables 1 and 2 [18,19]. Then, the finite element model and nodes were built and are shown in table 3.

Material	Elastic modulus	Poisson's ratio
Bone	7,300	0.3
Cartilage	12	0.42
Titanium alloy	110,000	0.3

Table 1: Properties of the bone and cartilage materials.

Ligament	Modulus of elasticity (MPa)	Poisson's ratio	Sectional area (mm2)	Stiffness (N/mm)
AtiF	260	0.4	18.4	141.8
PtiF	260	0.4	18.4	244.3
AtaFi	255.5	0.4	12.9	122.3
PtaFi	216.5	0.4	21.9	175.8
CaTi	512	0.4	9.7	126.6
AtiTa	184.5	0.4	13.5	141.8
PtiTa	99.5	0.4	22.6	244.3
TiCa	512	0.4	9.7	126.6
TiNa	320.7	0.4	7.1	44

Table 2: Material properties of the ligaments.

AtiF: Anterior Tibiofibular Ligament; PtiF: Posterior Tibiofibular Ligament; AtaFi: Anterior Talofibular Ligament; PtaFi: Posterior Talofibular Ligament; CaTi: Calcaneofibular Ligament; AtiTa: Anterior Tibial Ligament; PtiTa: Posterior Tibial Talus Ligament; TiCa: Tibiocalcaneal Ligament; TiNa: Tibionavicular Ligament

	Elements	Nodes
Tibia	37,876	61,152
Fibula	21,658	35,019
Talus	30,422	49,181
Calcaneus	47,126	74,773
Navicular	8,924	14,693
Screw	3,027	5,802
Forefoot	122,899	199,351
Implant	38,228	62,240

Table 3: Elements and nodes.

Finally, a finite element model of a healthy human foot was successfully established, and the following finite element models were established according to the requirements of the different fixation methods.

Boundary conditions and loads

There are many ways to divide a gait cycle, but it is usually divided into three phases: the heel-strike phase, the midstance phase and the push-off phase. The axis of flexion-extension and center of rotation were determined in this study according to the research methods reported by previous scholars [18,19]; the centers of the arcs of the tibialis and peroneal circumferences of the talus pulley were determined, and they were related to the two centers of the circle, the rotation axis, and the midpoint of the two centers of the circle, the rotation center. In research on stress during the gait cycle, the load is approximated to be relatively static. Stress during the gait cycle is simulated by applying loads of different sizes and directions. A contact pair is established between the articular surfaces with a coefficient of friction (no friction between the joint surface and titanium alloy prosthesis interface) of 0.01 [18,19]. Table 4 and figure 2 show the reference data for stress in different phases (Figure 2). The healthy model was consistent with previous studies.

	Heel-strike phase	Midstance phase	Push-off phase
Fx (N)	67.5	225	360
Fy (N)	562.5	907.5	810
Mz (N.m)	15.4	0	-112.5

Table 4: Finite element analysis parameters.

Fx: horizontal force (horizontal to forefoot), Fy: vertical force (vertical down), Mz: torque (positive value in that direction toward the lateral malleolus).

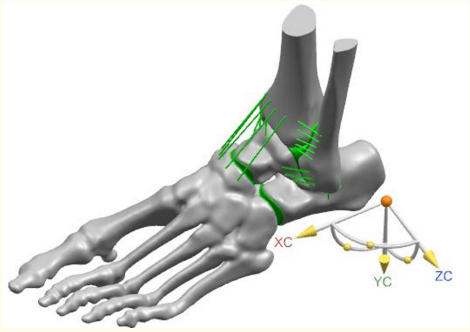

Figure 2: Schematic diagram of the load application direction in the finite element model.

Results

3D finite element models of talar prosthesis fixation with different methods were constructed and analyzed. The specifically constructed finite element model is shown in figure 3, and the distribution of pressure nephograms for the three different time phases of the healthy model is presented as an example in figure 4. The results regarding the pressures on the joints adjacent to the talus were as follows: 1. For the tibiotalar joint, the contact forces in the three phases were uniform under healthy conditions. After the talar prosthesis was implanted, the pressure significantly increased in the three phases, but the changes in the no fixation model were not significant. 2. For the subtalar joint, under healthy conditions, the pressure gradually increased in the heel-strike, midstance, and push-off phases in sequence. The trend was consistent after talar prosthesis replacement, and the fixation method without screws yielded results similar to those under the healthy state. When the subtalar joint was fixed, the pressure on the subtalar joint decreased significantly. Therefore, once the subtalar joint was fixed again, the range of motion of the hindfoot was further limited, and the subtalar joint pressure decreased again. 3. For the talar joint, the pressure values increased across the heel strike, midstance and push-off phases. The trend was consistent after talar prosthesis replacement. When screws were not used to fix the prosthesis, the pressure values in the midstance and push-off phases tended to increase. When screws were used to fix the subtalar joint, the pressure in the three phases of the talar joint decreased. When the talar joint was fixed again, the pressure value decreased further (Tables 5-7).

	Heel-strike	Midstance	Push-off
Healthy	3.5	4.6	5.1
Screw fixation of the subtalar joint	4.5 (+28.6%)	8.7 (+89.1%)	14.9 (+192.2%)
Screw fixation of the subtalar + talonavicular joint	4.2 (+20.0%)	7.6 (+65.2%)	13.6 (+166.7%)
Fixation without screws	3.9 (+11.4%)	5.6 (+21.7%)	11.1 (117.6%)

Table 5: Tibiotalar joint contact pressure/unit: MPa.

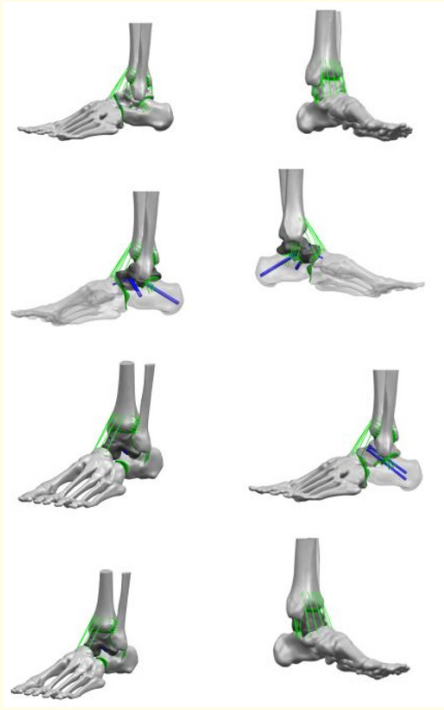

Figure 3: Model of a healthy person and three kinds of fixed models.

	Heel-strike	Midstance	Push-off
Healthy	0.4	4.3	9.8
Screw fixation of the subtalar joint	0.4 (+0%)	1.8 (-58.1%)	3.3 (-66.3%)
Screw fixation of the subtalar + talonavicular joint	0.2 (-50%)	0.4 (-90.7%)	1.9 (-84.9%)
Fixation without screws	0.4 (+0%)	4.5 (+4.7%)	13.5 (+37.8%)

Table 6: Subtalar joint contact pressure/unit: MPa.

Regarding slight movement in the adjacent talar joint, when a load was applied to simulate the three phases of the gait cycle, we compared the displacement of the talus relative to the adjacent joints, i.e., the tibia, calcaneus and navicular, and the results were as follows: The micromovement between joints was reduced by screw

	Heel-strike	Midstance	Push-off
Healthy	0.7	2.9	6.2
Screw fixation of the subtalar joint	0.7 (+0%)	1.9 (-34.5%)	2.9 (-53.2%)
Screw fixation of the subtalar + talonavicular joint	0.3 (-57.1%)	1.4 (-51.7%)	2.5 (-59.7%)
Fixation without screws	0.6 (-14.3%)	4.7 (+62.1%)	9.3 (+50%)

Table 7: Talonavicular joint contact pressure/unit: MPa.

fixation, and the situation was particularly obvious when the talus and subtalar joints were fixed. The displacement of the fixation without screw fixation of the talar prosthesis relative to the tibia was reduced, probably because the corresponding ligament-supporting connection was lost, but there was no significant increase in relative motion at either the subtalar joint or the talonavicular joint (Tables 8-10).

	Heel-strike	Midstance	Push-off
Healthy	0.4	1.1	1.9
Screw fixation of the subtalar joint	0.0 (-100%)	0.3 (-72.7%)	0.5 (-73.7%)
Screw fixation of the subtalar + talonavicular joint	0.0 (-100%)	0.1 (-90.9%)	0.2 (-89.5%)
Fixation without screws	0.3 (-25%)	0.9 (-18.2%)	1.5 (-21.1%)

Table 8: Movement relative to the tibia/unit: mm.

	Heel-strike	Midstance	Push-off
Healthy	0.1	0.4	0.6
Screw fixation of the subtalar joint	0.0 (-100%)	0.1 (-75%)	0.2 (-66.7%)
Screw fixation of the subtalar+ talonavicular joint	0.0 (-100%)	0.1 (-75%)	0.1 (-83.3%)
Fixation without screws	0.2(+100%)	0.5 (+100%)	0.7 (+16.7%)

Table 9: Movement relative to the calcaneus/unit: mm.

	Heel-strike	Midstance	Push-off
Healthy	0.1	0.4	0.7
Screw fixation of the subtalar joint	0.0 (-100%)	0.1 (-75%)	0.4 (-42.9%)
Screw fixation of the subtalar + talonavicular joint	0.0 (-100%)	0.1 (-75%)	0.1 (-85.7%)
Fixation without screws	0.1 (+0%)	0.6 (+50%)	0.9 (+28.6%)

Table 10: Movement relative to the navicular/unit: mm.

For the ankle joint range of motion, the pressure change between the peri-articular surfaces of the talus and the micromotion of the talus were measured, with the plane axis extending from the central axis of the second metatarsal bone to the heel and the central axis of the tibia used as a reference; the ankle joint was in the neutral position in the midstance phase, in dorsiflexion during the heel-strike phase, and in plantar flexion during the push-off phase. The ankle joint range of motion in the three phases was measured. The results showed that after total talar prosthesis replacement, the ankle joint range of motion changed. Screw fixation greatly limited the range of motion (consistent with the characteristics of fusion surgery). There was also limited range of motion in the model with fixation without screws, but this situation was the closest to the healthy situation (Table 11).

	Plantar flexion deg	Dorsiflexion deg
Healthy	8.6	13.2
Screw fixation of the subtalar joint	7.2 (-16.3%)	10.8 (-18.2%)
Screw fixation of the subtalar + talonavicular joint	6.9 (-19.8%)	10.4 (-21.2)
Fixation without screws	7.8 (-9.3%)	11.9 (-2.1%)

Table 11: Ankle joint range of motion/unit: degrees (°).

Discussion

The talus plays an important role in the biomechanics of the ankle. Abnormal anatomical structures have large effects on the function of the foot. The ankle joint bears a heavy load in the human body. Any injury to its anatomical structure will affect its stability.

Talus osteochondral injuries are common ankle joint injuries that considerably affect the ankle joint [20].

Ischemic collapse necrosis of the talus is challenging to treat [21,22]. To address this clinical challenge, there are currently three main therapeutic approaches: 1. Core decompression can preserve joint motion and effectively relieve pain, but the disadvantage is that it is suitable only for patients with early talus necrosis and is not effective for end-stage necrosis [23]. 2. Ankle joint fusion surgery has been suggested to relieve pain and is suitable for patients in almost all stages of necrosis, but it will greatly limit the range of motion of the ankle and affect the quality of life of patients [24]. After the talus collapses, structural bone grafting is often performed during fusion to prevent the force lines of the lower limbs from being affected. If the blood supply around the talus is extensively damaged, tibialis calcaneal fusion or posterior ankle arthrodesis is needed. However, for cases of severe collapse and necrosis of the talus, fusion surgery is not suitable, and in earlier studies, fusion surgery has been proven to be inferior to ankle prosthesis replacement in terms of mobility, efficacy and prognosis [25]. 3. Regarding ankle joint replacement for collapse necrosis of the talus, the requirement of residual bone mass of the talus is very high to reduce the probability of revision or refusion.

Whole talar prosthesis implantation was first performed and reported by Harnroongroj and Vanadurongwan [26] in 1997, but there were many postoperative complications due to limitations of the casting method. With the development of modern computer processing technology in recent years, 3D printing technology has been widely used in the clinical practice of orthopedics and has yielded good curative effects.

3D-printed, personalized all-talar prostheses can be used for collapse necrosis of the talus. The talus, the core of ankle-hind foot movement, has seven joint surfaces, so it is the first choice for personalized treatment. However, whether the whole talar prosthesis should be fixed after implantation is controversial. Regardless of whether the subtalar joint or subtalar joint is fused, the degree of flexibility and range of motion of the foot are affected [13]. If we choose not to fix the talar prosthesis [11,12] and use the bony structure of the talus between the ankle points and the ankle-foot complex to obtain self-stability, damage to the adjacent articular cartilage and complications such as prosthesis dislocation may occur. The clinical efficacy of different fixation methods has also been assessed in many studies. Due to the relatively short follow-up times and limited number of cases in this study, more scientific and objective data cannot be provided. Therefore, biomechanical studies are urgently needed to verify the biomechanical differences between several different fixation methods so that operators can select the best surgical method.

Traditional orthopedic biomechanical experiments (also gait analyses) are based mainly on animal or cadaver models. Although the results of these experiments are more reliable than those of simulations, it is often very difficult to obtain ideal experimental data without changing the physiological state of the model due to limitations in experimental methods, the need to adhere to ethical standards, and the influence of other factors. In recent years, with the development of medical imaging technology and computer processing technology, finite element analysis, a new biomechanical research method, has been widely used in orthopedic mechanics research. Simulation experiments performed using the finite element method have the advantages of a short experimental time, a low cost, the capability of simulating complex boundary conditions, the ability to provide comprehensive mechanical property testing, and good repeatability [14,15]. In this study, a finite element model was used to simplify and effectively simulate a healthy model and models of different methods of fixing a talar prosthesis.

It is traditionally believed that fixation must be performed after the prosthesis is inserted, which is similar to fusion surgery. The subtalar joint [13] needs to be fixed, or the navicular joint needs to be fixed simultaneously to stabilize the prosthesis at the ankle. For prosthesis-bone interfaces needing screw fixation, a special coating is often used to achieve the biomechanical effect of bone ingrowth. Professor Tang Kanglai conducted a series of studies on this topic and made clinical progress [27,28]. The operation is similar to fusion surgery. Hindfoot motion is limited to a certain extent, which was shown in the finite element model. When loads in different directions were applied, the range of motion of the talus relative to the screw-fixed joint surface decreased; during a simulated gait cycle, the pressure on the tibia-talus joint increased, and the pressure on the prosthesis-bone interface decreased. Screw fixation does limit the motion between joints and reduce the pressure between fusion joints; however, the finite element results showed that the reduced pressure is completely compensated by the tibialis joint. For the talus joint, there is not only a loss of range of motion and an increase in contact pressure but also an increased probabil-

ity of osteoarthritis in the talus joint surface and an increased possibility of late prosthesis loosening in the long term. However, the effect on ankle range of motion is similar to that of fusion surgery. Clinical research on total talus replacement with a prosthesis indicates that talar prostheses have a better curative effect in the short term [29]. However, studies on bone ingrowth between the bone and prosthesis interface and long-term clinical follow-up studies are currently underway.

Other scholars have used methods other than screw fixation. The first report of the use of an unfixed method was published by Assal and Stern [30] in 2004, and good curative effects were achieved within the five-year follow-up period. In the heel-strike phase of the gait cycle, when the ankle was in dorsiflexion, the talus was locked upward in the ankle, and there was a force component exerted vertically downward on the calcaneus; therefore, fixation was not needed. In the midstance phase, the upper surface of the talar prosthesis incurred downward stress from the tibia, which exerted a force against the calcaneus and navicular at an angle of 140°. The talus was relatively stable and did not need fixation. During the push-off phase, the ankle began to plantar flex, the hindfoot was locked, and the ankle was in the "unlocked state". The moment arm of the talus against the navicular increased, and fixation was not required [31]. The finite element model of this study also confirmed the assumption that talar prosthesis fixation without screws yields stable fixation, with biomechanical and ankle range of motion values closest to normal values. To the best of our knowledge, no one has conducted relevant studies on the self-stability of the talus in the past.

If screw fixation is used, the probability of prosthesis dislocation is relatively low. For cases without screw fixation, dislocation is possible in the following conditions. When the forefoot is off the ground, the Achilles tendon is pulled upward, the hindfoot is plantar flexed, the talus is unlocked forward, and the anterior ankle is loose. Then, the talus is displaced to a large extent forward and upward. Due to the containment effect of the navicular (bony structure) and the limiting effect of the tibialis anterior and anterior joint capsules (soft tissue) on the prosthesis, the probability of prolapse is relatively low, and the specific biomechanical mechanism needs to be studied further.

As has been verified in similar research, the finite element model established in this paper is a reliable model that can effectively reflect the biomechanical effects of different fixation methods after talus prosthesis implantation. By comparison, the use of screw fixation prostheses limits the ankle joint range of motion to a certain extent and changes its original biomechanical characteristics. Instead of using screw fixation of talar prostheses, fixation without screws is the closest to the normal fixation method.

Conclusion

Some shortcomings of this study were unavoidable. First, only the bony structures were simulated, and the soft tissues were simplified, which may affect the accuracy of this model to some extent with respect to real conditions. Second, the model was verified by repeating the experiments in previous studies, which does not yield the strongest form of evidence. Therefore, in the future, we plan to verify the results of this finite element study on clinical and cadaveric models. Finally, the surgical method of total talar prosthesis replacement should be carefully considered because the deep layer and the anterior peroneal ligament or the trigonal ligament cannot be reconstructed separately, thus leading to high requirements for the ankle joint bony structure.

Bibliography

1. Han Q., *et al.* "Measurement of talar morphology in northeast Chinese population based on three-dimensional computed tomography". *Medicine (Baltimore)* 98 (2019): e17142.

2. Timothy G. "Talus fracture". Treasure Island, FL: StatPearls Publishing (2020).

3. Flury A., *et al.* "Talar neck angle correlates with tibial torsion-Guidance for 3D and 2D measurements in total ankle replacement". *Journal of Orthopaedic Research* 39 (2021): 788-796.

4. Parekh SG and Kadakia RJ. "Avascular necrosis of the talus". *Journal of the American Academy of Orthopaedic Surgeons* 29 (2021): e267-278.

5. Oliva XM and Voegeli AV. "Aseptic (avascular) bone necrosis in the foot and ankle". *EFORT Open Reviews* 5 (2020): 684-690.

6. Jovic TH., *et al.* "3D bioprinting and the future of surgery". *Frontiers in Surgery* 7 (2020): 609836.

7. West TA and Rush SM. "Total talus replacement: case series and literature review". *The Journal of Foot and Ankle Surgery* 60 (2021): 187-193.

8. Huang J., *et al.* "Treatment of osteosarcoma of the talus with a 3D-printed talar prosthesis". *The Journal of Foot and Ankle Surgery* 60 (2021): 194-198.

9. Shnol H and LaPorta GA. "3D printed total talar replacement: a promising treatment option for advanced arthritis, avascular osteonecrosis, and osteomyelitis of the ankle". *Clinics in Podiatric Medicine and Surgery* 35 (2018): 403-422.

10. Scott DJ., *et al.* "Early outcomes of 3D printed total talus arthroplasty". *Foot and Ankle Specialist* 13 (2020): 372-377.

11. Kadakia RJ., *et al.* "3D printed total talus replacement for avascular necrosis of the talus". *Foot and Ankle International* 41 (2020): 1529-1536.

12. Tracey J., *et al.* "Custom 3D-printed total talar prostheses restore normal joint anatomy throughout the hindfoot". *Foot and Ankle Specialist* 12 (2019): 39-48.

13. Fang X., *et al.* "Total talar replacement with a novel 3D printed modular prosthesis for tumors". *Therapeutics and Clinical Risk Management* 14 (2018): 1897-1905.

14. Mehta S., *et al.* "Understanding the basics of computational models in orthopaedics: a nonnumeric review for surgeons". *Journal of the American Academy of Orthopaedic Surgeons* 25 (2017): 684-692.

15. Laz PJ and Browne M. "A review of probabilistic analysis in orthopaedic biomechanics". *Proceedings of the Institution of Mechanical Engineers, Part H* 224 (2010): 927-943.

16. O'Sullivan R., *et al.* "Crouch gait or flexed-knee gait in cerebral palsy: is there a difference? A systematic review". *Gait Posture* 82 (2020): 153-160.

17. Buckinx F., *et al.* "High intensity interval training combined with L-citrulline supplementation: effects on physical performance in healthy older adults". *Experimental Gerontology* 140 (2020): 111036.

18. Li J., *et al.* "Finite element analysis of the effect of talar osteochondral defects of different depths on ankle joint stability". *Medical Science Monitor* 26 (2020): e921823.

19. Lu CH., *et al.* "Establishment of a three-dimensional finite element model and stress analysis of the talus during normal gait". *Nan Fang Yi Ke Da Xue Xue Bao* 30 (2019): 2273-2276.

20. Georgiannos D., *et al.* "Osteochondral transplantation of autologous graft for the treatment of osteochondral lesions of talus: 5- to 7-year follow-up". *Knee Surgery, Sports Traumatology, Arthroscopy* 24 (2016): 3722-3729.

21. Horst F., *et al.* "Avascular necrosis of the talus: current treatment options". *Foot and Ankle Clinics* 9 (2004): 757-773.

22. Nunley JA and Hamid KS. "Vascularized pedicle bone-grafting from the cuboid for talar osteonecrosis: results of a novel salvage procedure". *The Journal of Bone and Joint Surgery American* 99 (2017): 848-854.

23. Sultan AA and Mont MA. "Core decompression and bone grafting for osteonecrosis of the talus: a critical analysis of the current evidence". *Foot and Ankle Clinics* 24 (2019): 107-112.

24. Taniguchi A., *et al.* "The use of a ceramic talar body prosthesis in patients with aseptic necrosis of the talus". *The Journal of Bone and Joint Surgery* 94 (2012): 1529-1533.

25. Valderrabano V., *et al.* "Kinematic changes after fusion and total replacement of the ankle: part 3: talar movement". *Foot and Ankle International* 24 (2003): 897-900.

26. Harnroongroj T and Vanadurongwan V. "The talar body prosthesis". *The Journal of Bone and Joint Surgery American* 79 (1997): 1313-1322.

27. Mu MD., *et al.* "Three-dimension printing talar prostheses for total replacement in talar necrosis and collapse". *International Orthopaedics* 45 (2021): 2313-2321.

28. Yang QD., *et al.* "Three-dimensional printed talar prosthesis with biological function for giant cell tumor of the talus: a case report and review of the literature". *World Journal of Clinical Cases* 9 (2021): 3147-3156.

29. Harnroongroj T and Harnroongroj T. "The talar body prosthesis: results at ten to thirty-six years of follow-up". *The Journal of Bone and Joint Surgery American* 96 (2014): 1211-1218.

30. Assal M and Stern R. "Total extrusion of the talus. A case report". *The Journal of Bone and Joint Surgery American* 86 (2004): 2726-2731.

31. Giddings VL., *et al.* "Calcaneal loading during walking and running". *Medicine and Science in Sports and Exercise* 32 (2000): 627-634.

Volume 5 Issue 9 September 2022